JOC The Journal of Organic Chemistry

Article

pubs.acs.org/joc

Kinetic Analysis and Mechanism of the Hydrolytic Degradation of Squaramides and Squaramic Acids

Marta Ximenis,[†] Emilio Bustelo,[‡] Andrés G. Algarra,[‡] Manel Vega,[†] Carmen Rotger,[†] Manuel G. Basallote,*[,‡] and Antonio Costa*[,†]

[†]Department of Chemistry, Universitat de les Illes Balears, Palma 07122, Spain

[‡]Department of Materials Scientist, Metallurgic Engineering and Inorganic Chemistry, Universidad de Cádiz, Puerto Real, 11510 Cádiz, Spain

Supporting Information

ABSTRACT: The hydrolytic degradation of squaramides and squaramic acids, the product of partial hydrolysis of squaramides, has been evaluated by UV spectroscopy at 37 °C in the pH range 3−10. Under these conditions, the compounds are kinetically stable over long time periods (>100 days). At pH >10, the hydrolysis of the squaramate anions shows first-order dependence on both squaramate and OH^-. At the same temperature and $[OH^-]$, the hydrolysis of squaramides usually displays biphasic spectral changes (A → B → C kinetic model) with formation of squaramates as detectable reaction intermediates. The measured rates for the first step ($k_1 \approx 10^{-4}$ M^{-1} s^{-1}) are 2−3 orders of magnitude faster than those for the second step ($k_2 \approx 10^{-6}$ M^{-1} s^{-1}). Experiments at different temperatures provide activation parameters with values of $\Delta H^{\ddagger} \approx 9-18$ kcal mol^{-1} and $\Delta S^{\ddagger} \approx -5$ to −30 cal K^{-1} mol^{-1}. DFT calculations show that the mechanism for the alkaline hydrolysis of squaramic acids is quite similar to that of amides.

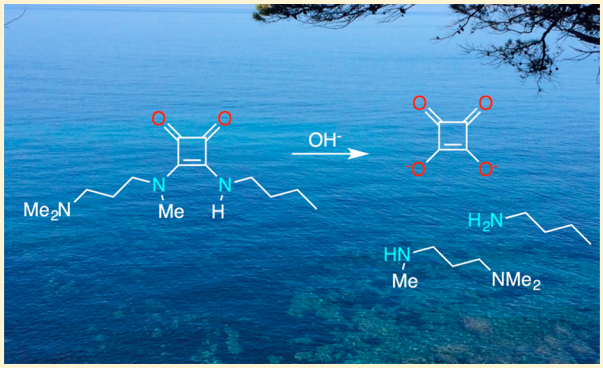

INTRODUCTION

3,4-Diamino derivatives of squaric acid, also known as squaramides, have received increasing attention in recent years.[1] Owing to their small size and relatively easy preparation, squaramides have found applications in diverse areas of chemistry such as molecular recognition,[2] supramolecular catalysis,[1d,3,4] materials science,[5] ion and molecular transport,[6] and sensing.[7] In the biological realm, squaramides have been used for specific cell labeling,[8] to prepare active bioconjugates,[9] or to replace the phosphate- and amide-type groups in bioisosteric replacements.[10] In medicinal chemistry, cell-penetrating squaramides are known to exhibit significant anticancer[11] and antiparasitic activity.[12]

There are evident similarities between squaramides and amides or ureas; the nitrogen atoms of a secondary squaramide are coplanar with the cyclobutendione ring. Their sp^2 hybridization is evidenced by a N−C(sp^2) bond length of 1.32 Å, which is significantly shorter than the single C(sp^3)−N bond of 1.46 Å (Figure 1a).[13] The measured barrier to rotation around the N−C(sp^2) bond is around 63 kJ mol^{-1}, which gives rise to the observation of *Z,Z* and *Z,E* conformers.[14] Squaramides are also known to show certain aromatic character[5c,15] and enhanced hydrogen-bonding capabilities as hydrogen bond donors[16,13] and acceptors,[7a,17] all in all resulting in compounds with excellent hydrolytic stability.

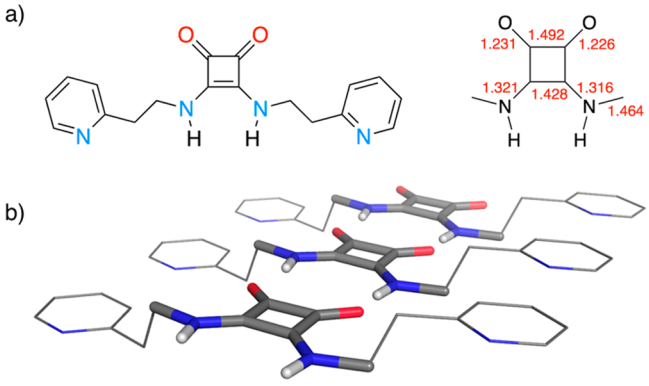

Figure 1. (a) X-ray bond lengths (Å) of a squaramide (CCDC 645873)[13] used as a model. (b) Perspective side view showing the planar arrangement of the squaramide units in the solid state and the two effective head-to-tail NH···O═C hydrogen bonds occurring between the squaramide units.

Despite the growing uses of squaramides and their unique properties, it is surprising that little is known about the physicochemical events underlying the fate and degradation of

Received: December 11, 2016
Published: January 20, 2017

DOI: 10.1021/acs.joc.6b02963
J. Org. Chem. 2017, 82, 2160−2170

squaramide-based compounds.[18] Knowledge of the hydrolytic stability and resistance to chemical degradation of squaramides is a relevant issue, with chemical and biomedical implications. In particular, a hydrolytic degradation pathway is likely to occur in bioactive squaramides and conjugates as part of the catabolism of these compounds.

In this work, we have examined the hydrolysis of several squaramides under biological conditions (37 °C, buffered aqueous solutions, 0.15 M ionic strength, $[H^+]$ or $[OH^-] < 10^{-2}$ M). Nevertheless, the reluctance of these compounds to hydrolysis has led us to strengthen the conditions when necessary ($0.01 < [H^+]$ or $[OH^-] < 1$ M), while keeping the temperature at 37 °C and raising the ionic strength to 1 M (NaCl).

RESULTS AND DISCUSSION

The full hydrolysis of squaramides produces squaric acid and two amines. Nevertheless, 3-hydroxy-4-amino derivatives of squaric acid, also known as squaramic acids, are formed as intermediates during hydrolysis. Hence, the kinetic data from the hydrolysis of squaramic acids are expected to provide valuable information about the rate law and hydrolysis rates in a simple manner. Furthermore, this allows us to assess the effect of the neighboring group: i.e., hydroxyl vs amide groups. For this reason, the kinetics of hydrolysis of several squaramic acids as a function of pH has been evaluated before facing the study of squaramides. In all cases, the kinetics were studied under pseudo-first-order conditions by monitoring the time-dependent changes in the UV–vis spectra of the corresponding squaramic acid or squaramide at 37 °C. The experiments were carried out at different pH values, and the apparent rate constants (k_{obs}) were calculated by performing global analyses of the absorption spectra acquired during the hydrolysis.[19]

At neutral pH, the squaramic acids **1**–**6** (Scheme 1) show intense absorption bands ($\varepsilon > 2 \times 10^4$ M^{-1} cm^{-1}) in the UV range with maximum absorptions at 276.0, 283.0, 274.0, 290.7, 294.0, and 308.0 nm, respectively. Under the same experimental conditions, the spectrum of the hydrolysis product, squaric acid, shows a band at λ_{max} 269.0 nm. Preliminary kinetic experiments showed that spectral changes are negligible when samples of squaramic acids **1**–**4** are incubated at 37 °C for several days in buffered solutions ranging from pH 4 to 10. Long-term experiments (40, 100, 190 days) carried out in screw-capped vials under the same experimental conditions also did not evolve into the squaric acid. Hence, it can be deduced that squaramic acids are kinetically stable toward hydrolysis in mildly acidic or basic media. However, hydrolysis of squaramic acids **1**–**4** occurs at 37 °C within a few days under more strongly alkaline conditions ($[OH^-] = 0.01$–1.00 M). The results clearly reveal the formation of the squarate anion in a single kinetic step as depicted in Figure 2a for compound **4** (10^{-5} M, $[OH^-] = 0.9$ M).

Scheme 1. Alkaline Hydrolysis of Squaramic Acids

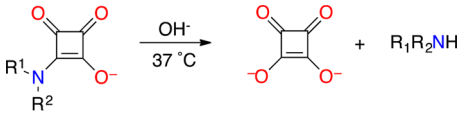

1 R^1 = n-Bu; R^2 = H
2 $R^1 = (CH_2)_3NMe_2$; R^2 = H
3 $R^1 = (CH_2)_3COOH$; R^2 = H
4 $R^1 = (CH_2)_3NMe_2$; R^2 = Me
5 R^1 = Ph; R^2 = H
6 $R^1 = R^2$ = *i*-Pr

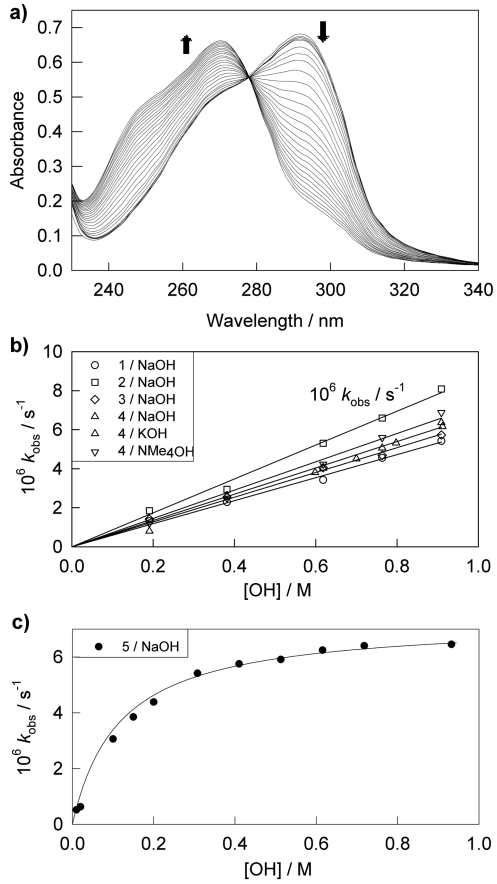

Figure 2. (a) Spectral evolution for the hydrolysis of a 10^{-5} M solution of **4** with 0.9 M NaOH (for clarity, only one out of three recorded spectra is shown). (b) k_{obs} vs $[OH]$ plots for **1**–**4**/NaOH, **4**/KOH, and **4**/NMe_4OH. (c) k_{obs} vs $[OH]$ plot for **5**/NaOH.

The observed rate constants (k_{obs}) show a linear dependence on the concentration of base (Figure 2b), thus excluding the ionization of the squaramidic NH hydrogen, as that would lead to a nonlinear dependence of k_{obs} on the hydroxide ion concentration.[20] The fit of the data to eq 1 leads to the second-order rate constants (k) included in Table 1. This shows that the reactivities of the squaramic acids **1**–**4** are very similar ($(5.9–8.7) \times 10^{-6}$ M^{-1} s^{-1}) regardless of the leaving group.

Table 1. Second-Order Rate Constant (k) for the Alkaline Hydrolysis of 1–6 at 37 °C

substrate/base	k_2, 10^{-6} M^{-1} s^{-1}
1/NaOH	5.9 ± 0.1
2/NaOH	8.7 ± 0.2
3/NaOH	6.3 ± 0.1
4/NaOH	6.7 ± 0.2
4/KOH	6.6 ± 0.1
4/NMe_4OH	7.3 ± 0.2
5/NaOH[a]	63 ± 8
6/NaOH	

[a]A pre-equilibrium constant of $K = 9 \pm 1$ M^{-1} was measured for this system.

DOI: 10.1021/acs.joc.6b02963
J. Org. Chem. 2017, 82, 2160–2170

However, compound **5** (R_1 = Ph) exhibits saturation kinetics (eq 2) on hydroxide concentration (Figure 2c), thus implying the existence of an initial acid−base equilibrium, with equilibrium constant K, in which OH^- abstracts a proton from the NH group and forms the conjugate base of **5**, which is unreactive against hydrolysis. Formation of the squarate anion occurs through reaction of the unmodified **5** with a rate constant k (eq 2) equivalent to the k value defined in eq 1.

$$k_{obs} = k[OH^-] \quad (1)$$

$$k_{obs} = \frac{k[OH^-]}{1 + K[OH^-]} \quad (2)$$

Equilibrium and rate constants can be obtained from the fitting to eq 2, and these show a faster hydrolysis rate (k = (63 ± 8) × 10^{-6} M^{-1} s^{-1}) and an equilibrium constant of 9 ± 1 M^{-1}.

A behavior similar to that of compound **5** has been reported for the alkaline hydrolysis of trichloroacetamide (CCl_3CONH_2) and trifluoroacetanilide ($CF_3CONHPh$), where K corresponds to the equilibrium constant for the ionization process caused by the enhanced acidity of these activated amides.[21] Thus, the observed rate equation for **5** can be explained by the formation of its conjugate base as an unreactive side product.[20,22] Finally, compound **6** does not appreciably hydrolyze under similar experimental conditions.

The rate constants for the hydrolysis of compounds **1**−**5** compare well with those reported for standard amides such as acetamide, *N*-methylacetamide, and *N*-ethylacetamide, which have alkaline hydrolysis constants of 4.71 × 10^{-5}, 5.46 × 10^{-6} and 3.10 × 10^{-6} M^{-1} s^{-1}, respectively, at 25 °C.[23] Thus, the anionic nature of the starting squaramate anion apparently does not interfere with the hydrolysis of the squaramide bond. Additionally, compound **4** was treated with KOH/KCl and NMe_4Cl/NMe_4OH, without a noticeable cation effect.

As squaramides derived from simple alkyl or aryl amines are insoluble in water, carbon chains containing solubilizing groups such as dimethylamino or carboxylic acid groups were introduced to fulfill this function (Chart 1). The spectra of the squaramides **7**−**14** show the absorption band slightly shifted toward higher wavelengths in comparison to squaramic acids **1**−**6**, the maximum being now observed in the range of 293−313 nm. Long-term experiments were again necessary to follow progress in the hydrolysis of the squaramides at 37 °C under buffered neutral (pH 4−10) and acidic conditions ([HCl] = 0.01−0.14 M). Experiments using samples of compound **10** at different pHs in sealed vials at 37 °C and measured after 40, 100, and 190 days only showed small changes at pH 9−10 and even minor changes at pHs lower than 2. Therefore, the hydrolysis of bis-squaramides requires stronger conditions under acidic (pH <2) than under alkaline conditions (pH >8).

The alkaline hydrolysis was then studied under conditions similar to those previously used for squaramates. As expected, the spectral changes observed are more complex than those found previously for the squaramates. Those for the hydrolysis of the antichagasic agent **10**[12b] are included in Figure 3. For compounds **7**−**11**, the evolution of the spectra with time corresponds to biphasic kinetics. The spectral changes are satisfactorily fitted to an A → B → C kinetic model with observed rate constants k_{1obs} and k_{2obs}.

The rates of both steps vary with the concentration of base, but the dependence is different in both cases. In the first step,

Chart 1. Chemical Structures of the Squaramides Investigated in This Work

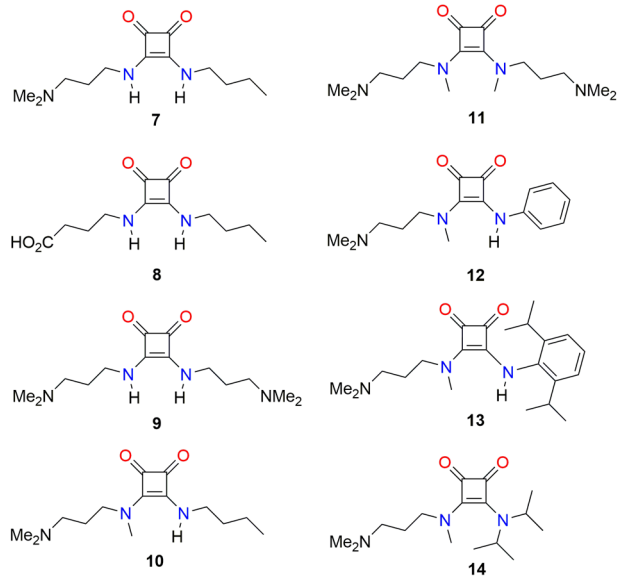

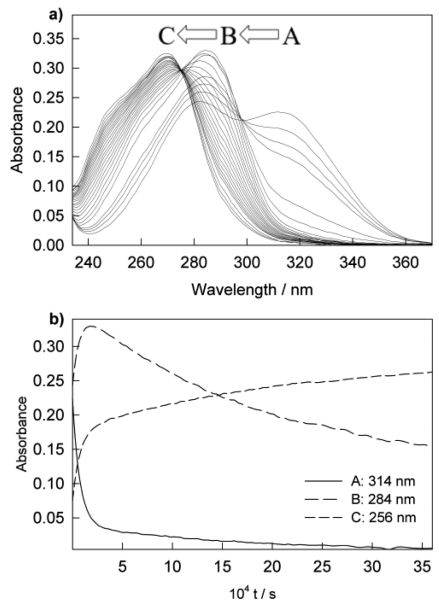

Figure 3. (a) Spectral changes with time observed during the hydrolysis of squaramide **10** at 37 °C in 0.9 M NaOH. For clarity, only one out of the three recorded spectra is shown. (b) Selected traces at various wavelengths.

saturation kinetics is observed (Figure 4a), and k_{1obs} values fit eq 2. The exception is compound **11**, lacking any ionizable NH group, for which k_{1obs} increases linearly with [OH^-] and the values can be fitted to eq 1 (Figure 4b). In the second step, k_{2obs} values satisfactorily fit eq 1 and yield the second-order hydrolysis rate constants k_2 included in Table 2.

The values of k_1, K, and k_2 for squaramides **7**−**14** are included in Table 2. Remarkably, the alkaline hydrolysis of trichloroacetamides, acetamides, and *N*-phenyl ureas, among others,[21a,23,24] show a nonlinear relationship between k_{1obs} and [OH^-] similar to that observed for **5**. The saturation kinetics observed in those cases is explained by the ionization of the NH groups of the amides or ureas, leading to unreactive conjugate bases at high pH. A similar interpretation is possible in the

DOI: 10.1021/acs.joc.6b02963
J. Org. Chem. 2017, 82, 2160−2170

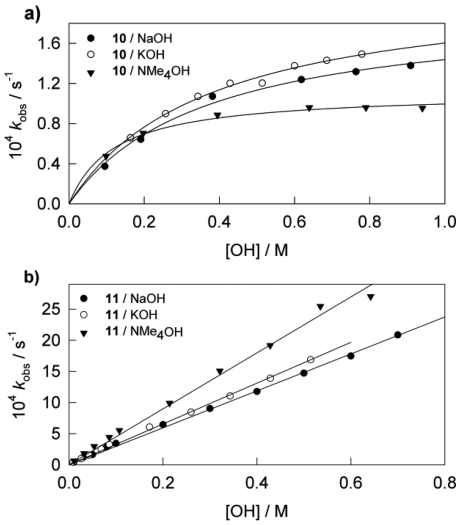

Figure 4. Plot of [OH^-] vs k_{1obs} for the hydrolysis of **10** (a) and **11** (b) in the presence of different salt/base combinations.

present case; the nature of the pre-equilibrium responsible for the saturation kinetics at high hydroxide ion concentration for **7**–**10** (and also for squaramate **5**) is likely related to the ionization of the squaramides bearing N–H groups (Scheme 2). The different rate law observed for **11**, which lacks NH groups and showed a linear dependence on [OH^-], gives further support to this interpretation.

The rate constants for the second resolved step match well with those obtained for the squaramate hydrolysis, with values of around 6×10^{-6} M^{-1} s^{-1}. A comparison between the first and second hydrolysis rate constants shows that the first hydrolysis step is roughly 2–3 orders of magnitude faster than the second step ($k_1 \gg k_2$). This effect is similar to the known difference in reactivity observed for the alkaline hydrolysis of phosphate triesters in comparison to anionic phosphate diesters.[24] The relative hydrolysis rates of certain diamides also show a similar trend. For instance, the alkaline hydrolysis of *cis*-maleamide at 65 °C is greater than that for acetamide by 2 orders of magnitude,[25] with the enhanced reactivity being explained on the basis of the electron-withdrawing ability of a second amide group. However, the same argument cannot be employed to explain the differences observed between squaramides and squaramate anions. Instead, it appears that the different rates of hydrolysis of the two squaramide groups have an electrostatic origin. The squaramate anion formed after the first hydrolysis has more difficulties in reacting readily with hydroxide or hydroxide–water cluster anions because of the electrostatic repulsion between the two negatively charged ions.

The k_1/k_2 ratios for compounds **7**–**9** are all close to 50, whereas compound **10** shows ratios between 84 and 114, with the value increasing with the size of the cation ($Na^+ < K^+ < NMe_4^+$) (Supporting Information). Compound **11** exhibits the greatest effect (452 for Na^+ and 612 for NMe_4^+). All in all, it seems that the presence of tetramethylammonium cations accelerates the first hydrolysis step in relation to the second step.

The introduction of aromatic substituents in compounds **12** and **13** provides an additional stabilization of charged species by both the cyclobutene and phenyl rings. The formation of an imidate anion causes compound **12** to evolve much more like a squaramic acid in terms of hydrolysis rate. In addition, the hydrolysis is directed toward the aliphatic amine group in spite of its slower hydrolysis, which is then followed by a fast aniline release in the second hydrolysis step.

An interesting aspect that deserves attention is the regioselectivity of the hydrolysis in unsymmetrical squaramides. The global analysis of the kinetic data is very useful in this regard, as it provides a calculated spectrum for the reaction intermediate that can be compared with the experimental spectra of the two possible squaramates. For instance, the calculated spectrum of the putative intermediate appearing during the alkaline hydrolysis of **10** shows a maximum at λ_{max} 285.5 nm and therefore does not coincide with either of the two available options, squaramates **1** (λ_{max} 276 nm) and **4** (λ_{max} 290.7 nm). This observation indicates that the recorded spectrum must be a combination of the spectra of these two squaramates (Figure S1 in the Supporting Information). Their relative abundances can actually be obtained by fitting the calculated spectrum to a linear combination of **1** and **4**, and the results indicate that the mixture is composed of 31% of **1** and 69% of **4**.

NMR experiments performed on the squaramide **10** (0.9 M NaOD/D_2O, 37 °C, 6 h) confirmed the formation of a mixture of squaramates as intermediates in the alkaline hydrolysis of unsymmetrical squaramides. Under these conditions, the concentration of the squaramate intermediates approaches a maximum. The resulting ^1H NMR spectrum matches well with the superposed spectra of **1**, **4**, and the corresponding free amines (Figure S2 in the Supporting Information). The integration of the characteristic squaramide NCH_2 signals (δ 3.25–3.50 ppm under alkaline conditions) provides a value of 55:45 for the **1**:**4** ratio, in reasonable agreement with the previous kinetic results. Although both approximations do not agree as to which is the dominant intermediate, it is clear that

Table 2. Kinetic Parameters for the Alkaline Hydrolysis (NaOH) of Squaramides 7–14

substrate[a]	k_1, 10^{-4} M^{-1} s^{-1}	K, M^{-1}	k_2, 10^{-6} M^{-1} s^{-1}	k_1/k_2
7	3.42 ± 0.02	3.98 ± 0.04	7.04 ± 0.05	49 ± 0.6
8	2.6 ± 0.2	3.2 ± 0.4	6.22 ± 0.09	42 ± 4
9	3.7 ± 0.2	4.6 ± 0.3	8.25 ± 0.05	45 ± 3
10	5.4 ± 0.5	2.7 ± 0.4	6.4 ± 0.2	84 ± 10
11	29.7 ± 0.3		6.57 ± 0.07	452 ± 9
12	0.141 ± 0.001			
13	0.004[b]			
14	15.1 ± 0.2			

[a]The kinetic measurements were carried out at 37 °C on 10^{-5} M solutions of the corresponding squaramides in H_2O (1 M NaCl). [b]The value of the rate constant for **13** is an estimation based on the NMR observations.

DOI: 10.1021/acs.joc.6b02963
J. Org. Chem. 2017, 82, 2160–2170

Scheme 2. Two-Step Alkaline Hydrolysis of a Representative Squaramide

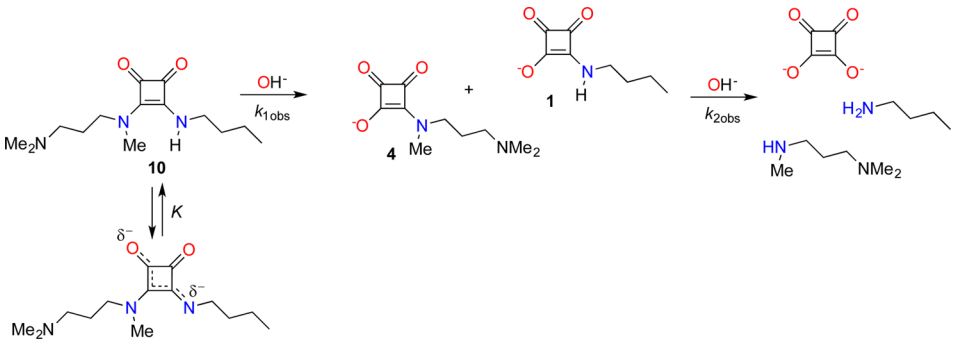

the rate constants for the hydrolysis of both C−N bonds are quite similar and that there is no preferred pathway for the first hydrolysis step. Regarding the hydrolysis of the squaramates, their rates are quite similar and, in the second kinetic step, the mixture of **1** and **4** would react with rate constants of 5.9×10^{-6} and 6.7×10^{-6} M^{-1} s^{-1}, respectively (see Table 1). However, because of the similarity between both constants, a single averaged value of 6.4×10^{-6} M^{-1} s^{-1} is observed for the second kinetic step in the hydrolysis of **10**.

In marked contrast to squaramides **7**−**11**, the hydrolysis of compound **12** takes place with monophasic kinetics, yielding the squarate dianion without any observable intermediate (Figure S3 in the Supporting Information). The spectral changes can be fitted to an A → B kinetic model, and the k_{1obs} vs [OH] plot shows a linear dependence on the hydroxide concentration (eq 1) with $k_1 = (1.41 \pm 0.01) \times 10^{-5}$ M^{-1} s^{-1}. NMR monitoring of the reaction in D_2O/NaOD confirms the absence of detectable intermediates. These results suggest that the hydrolysis of **12** takes place first at the aliphatic amine side (slow process) and then at the aniline group (fast), as indicated in Scheme 3. This hypothesis is further supported by the fact

Scheme 3. Alkaline Hydrolysis of the Phenyl-Substituted Squaramide 12

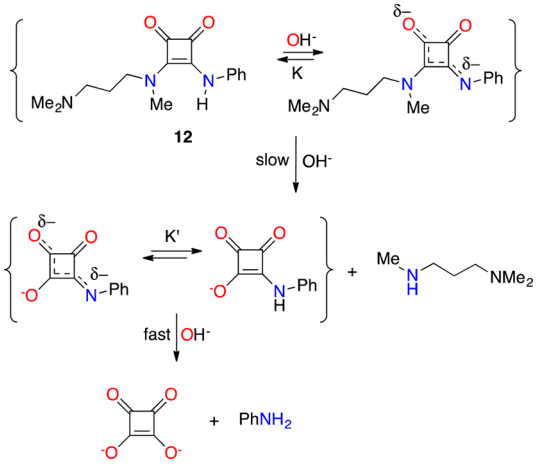

that the value of the rate constant for **5** in Table 1 is larger than the value of k_1 for **12** in Table 2. The hydrolysis kinetics of **12** is closer to that of the related squaramate **4** (aliphatic residue, $k = 0.67 \times 10^{-5}$ M^{-1} s^{-1}, eq 1) than to that of **5** (aromatic residue, $k = 6.3 \times 10^{-5}$ M^{-1} s^{-1}, eq 2).

Compound **13** represents another exception to the general behavior of squaramides. The introduction of two ^{i}Pr groups in the ortho positions of the aniline substituent effectively hinders the hydrolysis at both sides of the molecule, which remains unaltered under similar conditions and time frame (i.e., [OH] = 0.1−0.9 M, 37 °C, and 5.5 days).

After 3 weeks, NMR experiments show that only 20% of **13** is partially hydrolyzed at the aliphatic amine side, similarly to compound **12** but much slower. In agreement with the expectations from the behavior of other compounds, squaramide **14** undergoes hydrolysis at only one position to yield squaramate **6**, which is reluctant to hydrolyze under identical conditions when it is studied separately. The process takes place in a single kinetic step with observed rate constants linearly dependent on [OH^-].

Variable-temperature kinetic experiments allowed obtaining the activation parameters ($\Delta H^{‡}$ and $\Delta S^{‡}$) and the standard enthalpy and entropy of the pre-equilibrium using van't Hoff plots. Table S1 in the Supporting Information summarizes the activation parameters for compounds **7** and **9**−**11**. The results ($\Delta H^{‡} \approx 12$−16 kcal mol^{-1}, $\Delta S^{‡} \approx -19$ to -31 cal K^{-1} mol^{-1}) are similar to those reported for a series of diamides ($\Delta H^{‡} \approx 9$−18 kcal mol^{-1}, $\Delta S^{‡} \approx -5$ to -30 cal K^{-1} mol^{-1}): namely, oxalamide, malonamide, succinamide, and *cis*-/*trans*-maleamide.[25] This gives further support to the possibility of squaramides and amides sharing a similar hydrolysis mechanism with formation of steady-state tetrahedral intermediates such as **INT** in Scheme 4.[26]

Scheme 4. Structure of the Tetrahedral Intermediate (INT) Formed upon OH^- Attack

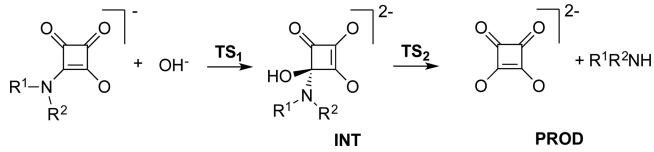

DFT Studies. While the hydrolysis of amides has been extensively studied from a computational viewpoint,[27] to our knowledge the mechanism of hydrolysis of squaramides and squaramic acids has never been analyzed in depth.[5c,28] Thus, to gain insight into the mechanism of the hydrolysis of squaramides, we carried out DFT calculations at the M06-2X//cc-pVTZ/PCM level of theory (for further information see the Supporting Information). We initially assumed that the alkaline hydrolysis of squaramates takes place via the tetrahedral intermediates II formed when the hydroxide anion attacks the C4 position of a squaramate anion.[29]

The calculations on compounds **1** and **6**, featuring secondary and tertiary alkyl amine groups, respectively, only led to minor

DOI: 10.1021/acs.joc.6b02963
J. Org. Chem. 2017, 82, 2160−2170

structural and energetic differences. These results were further confirmed by computing the hydrolysis of the model compounds **1t** and **6t**, in which the alkyl chains were replaced by methyl groups (Table S2 and Figure S4 in the Supporting Information). In all of these cases, the initial formation of the tetrahedral intermediates (**INT**) is thermoneutral ($\Delta G_{INT} \approx 0$ kcal mol^{-1}), taking place with barriers of ca. 13−15 kcal mol^{-1} (**TS$_1$**). The C−N bond breaking occurs in a subsequent step that is concerted with the proton transfer from the hydroxyl ligand to the departing amine (see **TS$_2$(1)** in Figure S4). This step is rate-determining and takes place with barriers of ca. 30 kcal mol^{-1}.

It is worth noting that the structures thus computed for the hydrolysis of **1**, **1t**, **6**, and **6t** are analogous to those calculated for the hydrolysis of amides.[27c] Especially relevant are those of the rate-determining second step (**TS$_2$**), all featuring additional four-membered rings due to the O−H···N interaction that allows the O to N proton transfer to be concerted with the C−N bond cleavage. Computational studies of the alkaline amide hydrolysis have shown that an ancillary water molecule, hydrogen-bonded to the tetrahedral intermediate, significantly decreases this **TS$_2$** barrier. The molecule of water acts as a bridge that facilitates the step due to the formation of more stable six-membered-ring transition states.[27] Importantly, a similar effect is observed when the alkaline hydrolysis of **1**, **1t**, **6**, and **6t** is computed in the presence of an explicit H_2O molecule. The associated energy values are included in Table 3, whereas Figure 5 shows the relevant structures for the hydrolysis of **1**·H_2O.

Table 3. Computed Relative Gibbs Free Energies of the Minima and Transition States Involved in the Hydrolysis of Squaramates Including an Explicit Water Molecule[a]

substrate	HBA	TS$_1$	INT	TS$_2$	PROD
1·H_2O	−12.6	5.5	−7.2	9.8	−34.8
1t·H_2O	−12.2	4.9	−7.3	8.8	−34.9
6·H_2O	−13.4	11.9	3.6	13.6	−35.1
6t·H_2O	−13.8	4.6	−5.6	9.1	−32.4
5·H_2O	−11.7	3.9	−7.6	5.2	−37.0
10t·H_2O-A[b]	−15.7	−5.9	−20.6	−7.8	−42.5
10t·H_2O-B[b]	−15.7	−6.8	−21.0	−8.3	−45.0

[a]Values are given in kcal mol^{-1}. Hydroxide anion and H-bonded [squaramate···OH_2] species are the reactants, whereas the released amine and [squarate···OH_2] species are computed as products. [b]The labels A and B correspond to the two alternative OH^- attacks on C3 or C4 carbons of the model squaramide **10t**, respectively.

The interaction between hydroxide and the hydrated squaramates leads to the formation of H-bonded adducts (**HBA**) that are ca. 12−15 kcal mol^{-1} more stable than the separate reactants. From these adducts, it is possible to generate the tetrahedral intermediates **INT** with **TS$_1$** barriers of ca. 18 kcal mol^{-1}, except for **6**, which shows a barrier of 25.3 kcal mol^{-1}. As expected, the explicit H_2O does not have an active role in the initial step of the hydrolysis, i.e. it is only H-bonded to the squaramate throughout the step, and therefore the barriers are close to those in Table S3 in the Supporting Information, again except for **6**.

In contrast, the data in Table 3 show that the inclusion of an explicit H_2O molecule in the calculations decreases the barrier for the second step of the hydrolysis significantly. At this level of theory, the hydrolysis (**TS$_2$**) adopts barriers of 10−17 kcal mol^{-1} (cf. 30 kcal mol^{-1} in the absence of the H_2O molecule). Such stabilization can be explained on the basis of the combination of that due to the H-bonding interactions, also appearing during the first step of the process, and the aforementioned catalyst effect of H_2O, which serves as a proton bridge and facilitates the concerted O to N proton transfer. The computed structure of **TS$_2$(1·H_2O)** in Figure 5 clearly exemplifies this catalytic role by presenting H···O distances between the hydroxyl group and the water molecule of 1.15 and 1.29 Å, indicative of an ongoing proton transfer process. Notably, the marked decrease in the computed **TS$_2$** barriers makes the formation of the tetrahedral intermediates (**TS$_1$**) rate determining, in agreement with the experimental results.

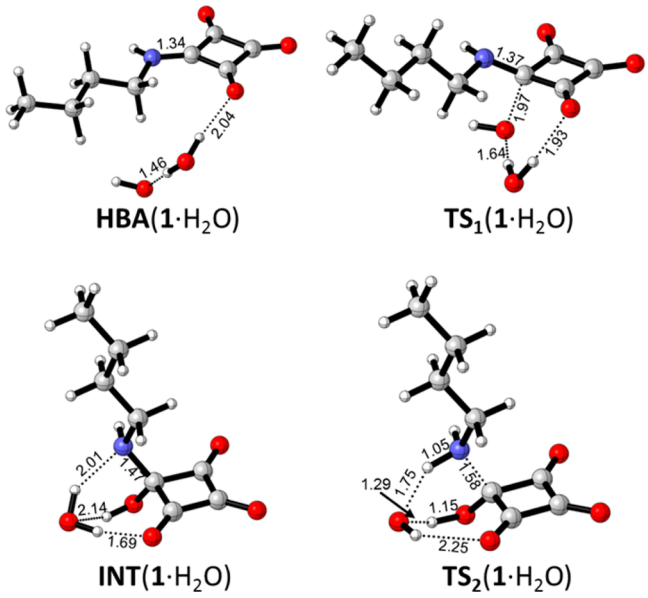

Figure 5. Perspective view of the DFT-optimized structures (M06-2X//cc-pVTZ/PCM) of **HBA(1·H_2O)**, **TS$_1$(1·H_2O)**, **INT$_1$(1·H_2O)**, and **TS$_2$(1·H_2O)**. Distances are given in Å.

Interestingly, the overall computed barrier for the alkaline hydrolysis of squaramate **6** is 27.0 kcal mol^{-1}, i.e., significantly larger than those of **1**, **1t** and **6t**, and is in agreement with the experimental observation of hindered hydrolysis of this compound. These thermochemical changes can be understood by the presence of the bulkier N(^{i}Pr)$_2$ amine. Specifically, the two ^{i}Pr chains in **TS$_2$(6·H_2O)** (Figure S5 in the Supporting Information) preclude the H-bonding interaction between the ancillary water molecule and the O atom at one of the neighboring C−O groups (d(H···O)= 2.25 Å).

Squaramate **5** (R_1 = Ph), whose alkaline hydrolysis also differs from that of **1** (R_1 = nBu), has been modeled in both the absence and presence of an ancillary H_2O molecule. The resulting free energies (Table S3 and Table 3) show similarities with those of compounds **1** and **6**. However, a crucial difference appears regarding the barrier for the second step. In the absence of explicit H_2O molecules, the thermodynamic differences between **TS$_2$(5)** and **TS$_2$(1)** follow the general trend: **TS$_2$(5)** is 14.7 kcal mol^{-1} above the separated reactants, whereas the value for **TS$_2$(1)** is 28.6 kcal mol^{-1}. As a consequence, the overall **TS$_2$** barrier for squaramate **5** is only 16.1 kcal mol^{-1}. Comparison of the structures of **TS$_2$(5)** (Figure S6 in the Supporting Information) and **TS$_2$(1)** (Figure S4 in the Supporting Information) allows tracing the origin of

DOI: 10.1021/acs.joc.6b02963
J. Org. Chem. 2017, 82, 2160−2170

the effect to the absence in $\mathbf{TS_2(5)}$ of the aforementioned O−H···N interaction (d(H···N)= 2.83 Å; cf. 1.74 Å in $\mathbf{TS_2(1)}$), which results in the four-membered ring required for the O to N proton transfer to be concerted with the C−N bond cleavage.[30] Here, the lower basicity of aniline in comparison to that of other departing amines[31] makes the concerted O to N proton transfer not required for the C−N bond cleavage to take place. As a consequence, the inclusion of a water molecule to model the alkaline hydrolysis of **5** does not result in the drastic thermodynamic changes computed for **1**, **1t**, **6**, and **6t**. Nonetheless, in line with the relatively fast alkaline hydrolysis of **5** (see Table 1), the calculated $\mathbf{TS_1}$ barrier for this compound in the presence of one explicit H_2O molecule is 15.6 kcal mol^{-1}: i.e., 2−3 kcal mol^{-1} lower than those for **1**, **1t**, **6**, and **6t** (Table 3).

The hydrolysis of the squaramides was computationally analyzed subsequently. Experimental work on the squaramide **10** has shown that the process involves the formation of two intermediates (squaramates **1** and **4**) with comparable rate constants and, therefore, they both should be formed with relatively similar barriers. To confirm this hypothesis, we computed the two possible pathways for the first hydrolysis in alkaline media of the model compound **10t** in the presence of one explicit H_2O molecule.

Similarly to the results for the alkaline hydrolysis of squaramates, the interaction of $\mathbf{10t{\cdot}H_2O}$ with hydroxide leads to the formation of the H-bonded adduct $\mathbf{HBA(10t{\cdot}H_2O)}$ that is 15.7 kcal mol^{-1} more stable than the separate reactants (see Figure 6). The attack of a hydroxide can take place

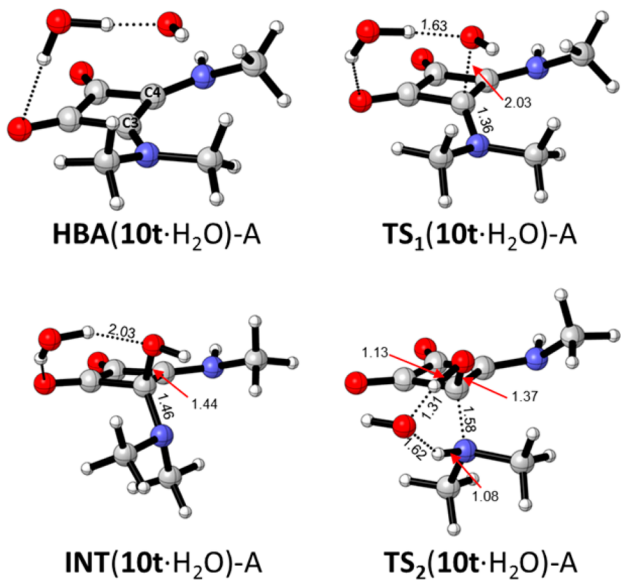

Figure 6. Perspective view of the DFT-optimized structures (M06-2X//cc-pVTZ/PCM) of $\mathbf{HBA(10t{\cdot}H_2O)}$-A, $\mathbf{TS_1(10t{\cdot}H_2O)}$-A, $\mathbf{INT_1(10t{\cdot}H_2O)}$-A and $\mathbf{TS_2(10t{\cdot}H_2O)}$-A. Alkyl groups were replaced by methyl groups. Distances are given in Å.

subsequently at either the C3 or C4 position of this squaramide, ultimately leading to the formation of the squaramates **1t** and **6t**, respectively. These two pathways have been labeled as A and B, respectively. The corresponding thermodynamic data are included in Table 3, whereas Figure 6 shows the structures computed for pathway A. The data indicate that the free energy profiles for pathways A and B are almost identical. Indeed, the $\mathbf{TS_1}$ barriers are 9.8 and 8.9 kcal/mol, respectively, whereas those for the second step ($\mathbf{TS_2}$) are 12.9 and 12.7 kcal/mol, respectively. These minor differences are surely within the computational errors, and so, the calculations suggest that the products resulting from both pathways, i.e. squaramates **1t** and **6t**, should both be observed as the products of the partial hydrolysis of **10t**. These observations give support to the initial hypothesis of the first alkaline hydrolysis of **10** not being regioselective: i.e., leading to a mixture of squaramates **1** and **6**. From a structural viewpoint, a comparison of the geometries for the first alkaline hydrolysis of $\mathbf{10t{\cdot}H_2O}$ in Figure 6 and that of $\mathbf{1{\cdot}H_2O}$ in Figure 5 shows little geometrical differences associated with the nature of the substituent at the adjacent carbon atom. The electronic consequences of this structural change are, however, significant, as the $\mathbf{TS_1}$ and $\mathbf{TS_2}$ barriers in $\mathbf{10t{\cdot}H_2O}$ are significantly lower than those for $\mathbf{6t{\cdot}H_2O}$, in agreement with the first hydrolysis of squaramides being 2−3 orders of magnitude faster than the second hydrolysis.

CONCLUSIONS

All in all, the studied squaramides and squaramate anions are kinetically stable at a temperature of 37 °C and pH range of 2−8. At pHs above 8 the hydrolysis of these compounds becomes observable. The present results demonstrate that the alkaline hydrolysis of squaramate anions proceeds with second-order kinetics and that the hydrolysis is relatively slow ($k \approx 10^{-6}$ M^{-1} s^{-1}) and unaffected by the existence of potentially interacting groups such as dimethylamino and carboxylate groups. On the other hand, the rate constants for the hydrolysis of the squaramides take place in two kinetically distinct steps. The first step ($k_1 \approx 10^{-4}$ M^{-1} s^{-1}) is ca. 10^2 times faster than the second step ($k_2 \approx 10^{-6}$ M^{-1} s^{-1}), with the latter values being comparable to those obtained for the corresponding squaramates. This general trend is not unexpected, since the second hydrolysis step of squaramides occurs on negatively charged squaramate anions. On these premises, and given the resemblance with the alkaline hydrolysis of amides,[26] a mechanism involving the formation of tetrahedral intermediates through the nucleophilic attack of a hydroxide ion to the C3 and C4 carbons of the squaramides can be proposed. This mechanism is supported by DFT calculations using a continuum-discrete solvation model. In addition to the kinetic and mechanistic details, the present results demonstrate the kinetic stability of squaramic acids and squaramides in aqueous solutions in a broad range of pH and must be useful to anyone planning to use them in the near future.

EXPERIMENTAL SECTION

The various chemicals were of commercial origin (Aldrich or Scharlau) and were used as received. ^{1}H, ^{13}C, and 2D NMR spectra (at 300 and 600 MHz) and ^{13}C (at 75 and 150 MHz) spectra were recorded on 300 and 600 MHz spectrometers in $CDCl_3$ or d_6-DMSO solutions at room temperature. The residual proton signal was used as a reference. Chemical shifts (δ) are given in ppm and coupling constants (J) in Hz. ESI-HRMS mass spectra were recorded on a magnetic sector or an Orbitrap mass spectrometer. Elemental analyses (C, H, N) were conducted by the "Centro de Microanálisis Elemental" of the "Universidad Complutense de Madrid" (Madrid, Spain).

Synthesis. The squaramic acids **1**−**4** and **6** were prepared by hydrolysis of the corresponding ethyl esters. Squaramic acid **5** was prepared according to a reported procedure.[32] The squaramides **7**−**11** were previously synthesized according to a modified procedure.[12b] Squaramides **12**−**14** are new compounds.

DOI: 10.1021/acs.joc.6b02963
J. Org. Chem. 2017, 82, 2160−2170

Typical Procedure for the Preparation of the Squaramic Acids 1−6.

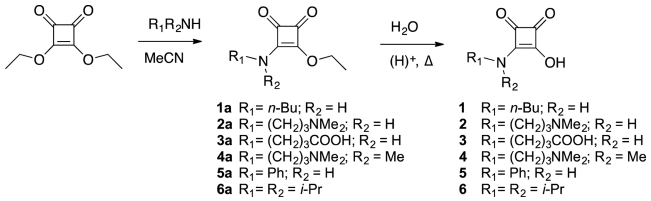

Diethyl squarate (500 mg, 2.94 mmol) in MeCN (3 mL) and 1 equiv of the corresponding amine were mixed in an oven-dried round-bottom flask. The mixture was stirred under nitrogen at room temperature (**1a**, **2a**) for 10 h or at higher temperatures for a variable period (see below). The crude mixture was then concentrated under reduced pressure and purified by column chromatography on silica gel with CH_2Cl_2/MeOH (95/5 v/v) or CH_2Cl_2/EtOAc (90/10 v/v) as eluent to afford the squaramic acid ethyl esters **1a**−**6a**. Next, the esters (500 mg) were digested with water at 90 °C for 8−20 h (Milli-Q, 15−20 mL), with or without added acid, recovering the resulting solid acids **1**−**4** and **6** by filtration.

*3-(Butylamino)-4-ethoxycyclobut-3-ene-1,2-dione (**1a**).*[14] White amorphous solid, 562 mg, yield 97%. Mp: 49−50 °C. ^{1}H NMR ($CDCl_3$): δ 6.42 (br s, 0.74H), 5.32 (br s, 0.26H), 4.76 (q, J = 6.9 Hz, 2H), 3.65(br, 0.58H), 3.42(br q, J = 6.6 Hz, 1.53H), 1.59 (m, 2H), 1.44 (t, J = 6.9 Hz, 3H), 1.36(m, 2H), 0.92 (t, J = 7.2 Hz, 3H). ^{13}C NMR ($CDCl_3$): δ 189.9, 182.8, 177.6, 172.6, 69.8, 44.8, 32.8, 19.7, 16.0, 13.8. ESI(+)-HRMS:: m/z (%) calcd for $C_{10}H_{15}NO_3Na$ [M + Na]$^+$ 220.0941; found 220.0936.

*3-((3-(Dimethylamino)propyl)amino)-4-ethoxycyclobut-3-ene-1,2-dione (**2a**).*[14] Yellow amorphous solid, 599 mg, yield 90%. Mp: 56−59 °C. ^{1}H NMR ($CDCl_3$): δ 7.76 (br s, 0.6H), 7.58 (br s, 0.4H), 4.73 (q, J = 6.9 Hz, 2H), 3.78 (br t, 0.7H), 3.54 (br t, J = 6 Hz, 1.3H), 2.43 (br t, J = 5.7 Hz, 2H), 2.22 (s, 6H), 1.73 (m, 2H), 1.42 (t, J = 6.9 Hz, 3H). ^{13}C NMR ($CDCl_3$): δ 189.5, 183.2, 177.3, 172.6, 69.6, 58.8, 58.3, 45.4, 44.9, 26.8, 16.9. ESI(+)-HRMS: m/z (%) calcd for $C_{11}H_{19}N_2O_3$ [M + H]$^+$ 227.1390; found 227.1389.

*4-((2-Ethoxy-3,4-dioxocyclobut-1-en-1-yl)amino)butanoic Acid (**3a**).*[38] To a solution of diethyl squarate (500 mg, 2.94 mmol) and 4-aminobutyric acid (313 mg, 2.94 mmol) in MeCN (10 mL) was added DIPEA (1.05 mL). The mixture was stirred at 50 °C for 15 h. The crude mixture was concentrated and diluted with water (12 mL) and HCl 3 N (3 mL). The resulting solution was extracted with EtOAc (10 × 10 mL). The combined EtOAc extracts were washed with brine and dried over Na_2SO_4. The solvent was removed under reduced pressure to give a yellow solid, 599 mg, yield 90%. Mp: 56−59 °C. ^{1}H NMR ($CDCl_3$): δ 7.76 (br s, 0.6H), 7.58 (br s, 0.4H), 4.73 (q, J = 6.9 Hz, 2H), 3.78 (br t, 0.7H), 3.54 (br t, J = 6 Hz, 1.3H), 2.43 (br t, J = 5.7 Hz, 2H), 2.22 (s, 6H), 1.73 (m, 2H), 1.42 (t, J = 6.9 Hz, 3H). ^{13}C NMR ($CDCl_3$): δ 189.5, 183.2, 177.3, 172.6, 69.6, 58.8, 58.3, 45.4, 44.9, 26.8, 16.0. ESI(−)-HRMS m/z (%) calcd for $C_{10}H_{12}NO_5$ [M − H]$^-$ 226.07210; found 226.0717; ESI(+)-HRMS: m/z (%) calcd for $C_{10}H_{13}NO_5Na$ [M + Na]$^+$ 250.06859; found 250.0682.

*3-((3-(Dimethylamino)propyl)(methyl)amino)-4-ethoxycyclobut-3-ene-1,2-dione (**4a**).*[12b] To a solution of diethyl squarate (500 mg, 2.94 mmol) in MeCN (15 mL) was added *N*,*N*,*N*′-trimethyl-1,3-propanediamine (341.6 mg, 2.94 mmol). The mixture was stirred at room temperature for 3 h. The crude mixture was concentrated and the residue purified by column chromatography (silica gel, CH_2Cl_2/MeOH (80/20 v/v)) to give a yellow oil, 692 mg, yield 98%. ^{1}H NMR ($CDCl_3$): δ 4.76 (q, J = 7.2 Hz, 1H), 4.75 (q, J = 7.2 Hz, 1H), 3.72 (t, J = 7.2 Hz, 1H), 3.44 (t, J = 7.2 Hz, 1H), 3.34 (s, 1.5H), 3.15 (s, 1.5H), 2.33 (m, 2H), 2.24 (s, 3H), 2.22 (s, 3H), 1.81 (m, 2H), 1.45 (t, J = 7.2 Hz, 1.5 H), 1.44 (t, J = 7.2 Hz, 1.5 H) ppm. ^{13}C NMR (75 MHz, $CDCl_3$): δ 188.3, 188.0, 181.5, 175.6, 175.5, 171.65, 171.3, 68.7, 55.4, 49.7, 49.0, 44.4, 36.0, 35.6, 25.0, 24.8, 15.2 ppm. ESI(+)-HRMS: m/z (%) calcd for $C_{12}H_{21}N_2O_3Na$ [M + H]$^+$ 241.1552; found 241.1557.

*3-(Ethoxy)-4-(phenylamino)cyclobut-3-ene-1,2-dione (**5a**).*[39] To a solution of diethyl squarate (500 mg, 2.94 mmol) in MeCN (15 mL) was added aniline (275 mg, 2.95 mmol). The mixture was stirred at 80 °C for 24 h to give a yellow-orange solid that was isolated by filtration. The crude solid was digested at room temperature with hexane/ethanol (92/8 v/v; 20 mL) and hexane (2 × 20 mL) and filtered to give a yellow solid, 500 mg, yield 78%. Mp: 111−114 °C. ^{1}H NMR ($CDCl_3$): δ 8.04 (br s, 1H), 7.32 (m, 4H), 7.15 (m, 1H), 4.88 (q, J = 7.2 Hz, 2H), 1.50 (t, J = 7.2 Hz, 3H). ^{13}C NMR ($CDCl_3$): δ 189.0, 184.1, 178.3, 168.8, 137.2, 129.7, 125.1, 119.5, 70.6, 16.1.

*3-(Diisopropylamino)-4-ethoxycyclobut-3-ene-1,2-dione (**6a**).*[40] To a solution of diethyl squarate (500 mg, 2.94 mmol) in MeCN (15 mL) were added *N*,*N*-diisopropylamine (598 mg, 5.90 mmol) and DIPEA (1.05 mL). The mixture was stirred at 50 °C for 24 h. The crude mixture was concentrated and the residue purified by column chromatography (silica gel) to give a yellow solid, 630 mg, yield 95%. Mp: 77−79 °C. ^{1}H NMR ($CDCl_3$): δ 4.82 (q, J = 7.2 Hz, 2H), 4.63 (br m, 1H), 3.93 (m, 1H), 1.45 (t, J = 7.2 Hz, 3H), 1.29 (d, J = 6.6 Hz, 6H) + 1.28 (d, J = 6.9 Hz, 6H). ^{13}C NMR ($CDCl_3$): δ 189.1, 182.6, 175.7, 171.3, 69.6, 50.0, 48.8, 22.1, 21.9, 16.1. ESI(+)-HRMS: m/z (%) calcd for $C_{12}H_{19}NO_3Na$ [M + Na]$^+$ 248.1257; found 248.1252.

*3-(Butylamino)-4-hydroxycyclobut-3-ene-1,2-dione (**1**).*[32] Obtained as the free acid from a mixture of **1a** (500 mg), water (30 mL), and HCl (3 N, 1 mL). White solid, 367 mg, yield 86%. Mp: 165 °C dec. ^{1}H NMR (DMSO-d_6): δ 8.32 (br t, 1H), 3.38 (q, J = 6.6 Hz, 2H), 1.49 (m, 2H), 1.28 (m, 2H), 0.87 (t, J = 7.2 Hz, 3H). ^{13}C NMR (DMSO-d_6): δ 185.6, 184.9, 183.7, 174.4, 43.7, 32.9, 19.5, 14.0. ESI(−)-HRMS m/z (%) calcd for $C_8H_{10}NO_3$ [M − H]$^-$ 168.06572; found 168.06527. ESI(+)-HRMS: m/z (%) calcd for $C_8H_{11}NO_3Na$ [M + Na]$^+$ 192.06314; found 192.06311.

*3-((3-(Dimethylamino)propyl)amino)-4-hydroxycyclobut-3-ene-1,2-dione (**2**).* Pale ochre amorphous solid 430 mg, yield 98%. Mp: 204−207 °C. ^{1}H NMR (DMSO-d_6): δ 7.16 (t, J = 6.3 Hz, 1H), 3.42 (q, J = 6 Hz, 2H), 3.06 (t, J = 6.9 Hz, 2H), 2.75 (s, 6H), 1.83 (m, 2H). ^{13}C NMR (D_2O): δ 197.2, 191.1, 183.9, 57.6, 45.4, 43.2, 28.5. ESI(+)-HRMS: m/z (%) calcd for $C_9H_{14}N_2O_3Na$ [M + Na]$^+$ 221.0897; found 221.0887.

*4-((2-Ethoxy-3,4-dioxocyclobut-1-en-1-yl)amino)butanoic Acid (**3**).* Obtained from a mixture of **1a** (500 mg), water (30 mL), and HCl (3 N, 3 mL). The crude solution was extracted with EtOAc (10 × 10 mL). The combined EtOAc extracts were washed with brine and dried with Na_2SO_4. Removal of the solvent afforded **3** as a white solid, 122 mg, yield 28%. Mp: 157−159 °C dec. ^{1}H NMR (DMSO-d_6): δ 8.28 (br t, 1H), 3.39 (q, J = 6.3 Hz, 2H), 2.25 (t, J = 7.2 Hz, 2H), 1.74 (m, 2H). ^{13}C NMR (DMSO-d_6): δ 185.2, 184.5, 183.1, 174,0 173.9, 43.0, 30.6, 25.7. ESI(−)-HRMS m/z (%) calcd for $C_8H_8NO_5$ [M − H]$^-$ 198.04080; found 198.0401.

*3-((3-(Dimethylamino)propyl)(methyl)amino)-4-hydroxycyclobut-3-ene-1,2-dione (**4**).* Obtained following the general procedure. Then, the crude solid was digested with hot ethyl ether (3 × 15 mL). White solid, 433 mg, yield 98%. Mp: >250 °C dec. ^{1}H NMR (D_2O): δ 3.75 (t, J = 6.6 Hz, 2H), 3.29 (s, 3H), 3.23−3.18 (t, J = 7.7 Hz, 2H), 2.91 (s, 6H), 2.13 (m, 2H). ^{13}C NMR (D_2O): δ 196.1, 190.5, 183.0, 57.3, 50.3, 45.4, 38.2, 25.0. ESI(+)-HRMS: m/z (%) calcd for $C_{10}H_{17}N_2O_3$ [M + H]$^+$ 213.1239; found 213.1238. Anal. Calcd for $C_{10}H_{16}N_2O_3$: C, 56.59; H, 7.60; N, 13.20. Found: C, 56.10; H, 7.30; N, 13.03.

*3-(Hydroxy)-4-(phenylamino)cyclobut-3-ene-1,2-dione (**5**).* Obtained as described in the literature by microwave irradiation of a mixture of squaric acid and aniline.[32]

*3-(Diisopropylamino)-4-ethoxycyclobut-3-ene-1,2-dione (**6**).* Crystalline white solid, quantitative yield. Mp: >210 °C dec. ^{1}H NMR (DMSO-d_6): δ 10.31 (br s, 1H), 4.32 (m, 2H), 1.25 (d, J = 6.9 Hz, 12H). ^{13}C NMR (D_2O): δ 193.7, 189.4, 182.2, 51.8, 23.9. ESI-FTMS m/z (%) calcd for $C_{10}H_{16}O_3N$ [M + H]$^+$ 198.1125; found 198.1125. ESI(−)-HRMS m/z (%) calcd for $C_{10}H_{14}O_3N$ [M − H]$^-$ 196.0979; found 196.0973. Anal. Calcd for $C_{10}H_{15}NO_3$: C, 60.90; H, 7.67; N, 7.10. Found: C, 60.73; H, 7.43; N, 7.06.

DOI: 10.1021/acs.joc.6b02963
J. Org. Chem. 2017, 82, 2160−2170

General Procedure for the Preparation of the Squaramic Acids 7−11.

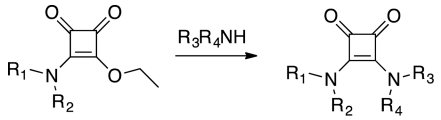

7 R_1 =$(CH_2)_3NMe_2$; R_2=H; R_3= n-Bu; R_4=H
8 R_1=$(CH_2)_3COOH$; R_2=H; R_3 =nBu; R_4=H
9 R_1 =$(CH_2)_3NMe_2$; R_2=H; R_3 =$(CH_2)_3NMe_2$; R_4=H
10 R_1= $(CH_2)_3NMe_2$; R_2 = Me; R_3 =nBu; R_4=H
11 R_1 =$(CH_2)_3NMe_2$; R_2= Me; R_3 =$(CH_2)_3NMe_2$; R_4=Me
12 R_1 = Ph; R_2= H; R_3 =$(CH_2)_3NMe_2$; R_4=Me
13 R_1 =$(iPr)_2$ Ph; R_2=Me; R_3 =$(CH_2)_3NMe_2$; R_4=Me
14 R_1 = iPr; R_2=IPr; R_3 =$(CH_2)_3NMe_2$; R_4=Me

The squaramides **7**−**11** were prepared following a modified procedure described previously by us,[12b] from equimolar mixtures of diethyl squarate (500 mg, 2.94 mmol) and the corresponding R_1R_2NH neat amine. Alternatively, the above mixture was dissolved in a minimum volume of MeCN or EtOH and stirred for 3 h at room temperature. After this period, the R_3R_4NH amine (2.97 mmol) was added and the resulting mixture heated further with stirring for several hours. After it was cooled to room temperature, the crude mixture was purified by column chromatography or by selective precipitation.

*3-(Butylamino)-4-((3-(dimethylamino)propyl)(methyl)amino)-cyclobut-3-ene-1,2-dione (**7**).*[12b] R_1R_2NH = *N*,*N*-dimethyl-1,3-propanediamine (374 μL, 2.94 mmol); R_3R_4NH = *n*-butylamine (295 μL, 2.97 mmol). The resulting solid was diluted with MeCN (5 mL), filtered, and washed with MeCN (3 × 10 mL). White solid, 535 mg, yield 72%.

*4-((2-(Butylamino)-3,4-dioxocyclobut-1-en-1-yl)amino)butanoic Acid (**8**).*[12b] R_1R_2NH = 4-aminobutyric acid (313 mg, 2.94 mmol) and DIPEA (1.05 mL, 6 mmol) in MeCN (10 mL) were stirred at 50 °C for 8 h. Next, R_3R_4NH = *n*-butylamine (350 μL, 3.5 mmol) was added to the mixture, which was then stirred at 50 °C for 50 h. After solvent removal in vacuo, the residue was dissolved in water and acidified with HCl (1 N) to pH 2 to afford **8** as a white solid that was collected by filtration, 630 mg, yield 84%.

*3,4-Bis((3-(dimethylamino)propyl)amino)cyclobut-3-ene-1,2-dione (**9**).*[12b] R_1R_2NH = R_3R_4NH = *N*,*N*-dimethyl-1,3-propanediamine (860 μL, 6.76 mmol) in 3 mL of EtOH. The mixture was stirred for 15 h at room temperature. After solvent removal under vacuum, the residue was washed with MeCN (3 × 10 mL). White amorphous solid, 621 mg, yield 75%.

*3-(Butylamino)-4-((3-(dimethylamino)propyl)(methyl)amino)-cyclobut-3-ene-1,2-dione (**10**).*[12b] R_1R_2NH = (N,N,N′-trimethyl-1,3-propanediamine (450 μL, 2.94 mmol); R_3R_4NH = *n*-butylamine (295 μL, 2.97 mmol). CC (neutral Al_2O_3; first CH_2Cl_2, then CH_2Cl_2/MeOH 95/5 v/v). White waxy solid 770 mg, yield 98%.

*3,4-Bis((3-(dimethylamino)propyl)(methyl)amino)cyclobut-3-ene-1,2-dione (**11**).*[12b] R_1R_2NH = R_3R_4NH = *N*,*N*,*N*′-trimethyl-1,3-propanediamine (1.03 mL, 6.82 mmol) neat. The mixture was stirred for 15 h at room temperature. The residue was purified by CC (neutral Al_2O_3). White waxy solid, 826 mg, yield 90%. Mp: 43−45 °C. ^{1}H NMR ($CDCl_3$): δ 3.71 (t, *J* = 7.5 Hz, 4H), 3.17 (s, 6H), 2.30 (t, *J* = 7.2 Hz, 4H), 2.22 (s, 12H), 1.81 (m, 4H). ^{13}C NMR ($CDCl_3$): δ 184.2, 169.4, 56.6, 51.4, 45.7, 39.8, 26.47. ESI(+)-HRMS: *m*/*z* (%) calcd for $C_{16}H_{31}N_4O_2$ $[M + H]^+$ 311.2447; found 311.2448.

*3-((3-(Dimethylamino)propyl)(methyl)amino)-4-(phenylamino)-cyclobut-3-ene-1,2-dione (**12**).* To a solution of the squaramic acid ethyl ester **5a** (500 mg, 2.3 mmol) in EtOH (15 mL) was added neat *N*,*N*,*N*′-trimethyl-1,3-propanediamine (390 μL, 2.53 mmol). The mixture was stirred at 80 °C for 48 h. After solvent removal in vacuo, the residue was purified by CC (silica gel) to afford **12** as a white solid, 507 mg, yield 77%. Mp: 132−134 °C. ^{1}H NMR (CD_2Cl_2): δ 10.64 (br s, 1H), 7.31 (t, *J* = 7.2 Hz, 2H), 7.2 (d, *J* = 7.5 Hz, 2H), 7.01 (t, *J* = 7.2 Hz, 1H), 3.5 (br t, *J* = 5.1 Hz, 2H), 3.37 (s, 3H), 2.45 (br t, *J* = 5.1 Hz, 2H), 2.3 (s, 6H), 1.83 (br m, 2H). ^{13}C NMR (CD_2Cl_2): δ 186.0, 182.1, 171.3, 164.5, 139.9, 129.3, 122.8, 118.9, 54.3, 48.1, 44.8, 35.9, 22.9. ESI(+)-HRMS: *m*/*z* (%) calcd for $C_{16}H_{22}N_3O_2$ $[M + H]^+$ 288.1712; found 288.1709.

*3-((2,6-Diisopropylphenyl)amino)-4-((3-(dimethylamino)propyl)-(methyl)amino)cyclobut-3-ene-1,2-dione (**13**).* Diethyl squarate (500 mg, 2.94 mmol) and 2,6-diisopropylaniline (1.21 mL, 5.9 mmol) were heated at 100 °C with stirring for 48 h. The dilution of the resulting oil with CH_2Cl_2 (10 mL) induced the precipitation of the double diisopropylaniline squaramide (140 mg). This solid was washed with CH_2Cl_2 (3 × 5 mL). The combined CH_2Cl_2 extracts were purified by CC (silica gel) to give an oily product which was treated with pentane to induce the precipitation of the ethyl ester **13a**, 406 mg, yield 46%. Mp: 155−157 °C. ^{1}H NMR ($CDCl_3$): δ 7.36 (t, *J* = 7.8 Hz, 1H), 7.18(d, *J* = 7.5 Hz, 2H), 6.95 (br s, 1H), 4.57 (q, *J* = 6.9 Hz, 2H), 3.07 (m, 2H), 1.23 (t, *J* = 7.2 Hz, 3H), 1.19 (d, *J* = 6.9 Hz, 12H). ^{13}C NMR ($CDCl_3$): δ 189.5, 184.1, 179.2, 172.5, 146.4, 131.2, 129.4, 123.7, 69.7, 28.8, 23.7, 15.8. ESI(+)-HRMS: *m*/*z* (%) calcd for $C_{36}H_{46}N_2O_6Na$ $[2M + Na]^+$ 625.3254; found 625.3251. Anal. Calcd for $C_{18}H_{23}NO_3$: C, 71.73; H, 7.69; N, 4.65. Found: C, 71.63; H, 7.41; N, 4.88.

A solution of **13a** (500 mg, 1.66 mmol) and *N*,*N*,*N*′-trimethyl-1,3-propanediamine (304 μL, 1.99 mmol) in EtOH (15 mL) was heated with stirring at 50 °C for 24 h. After solvent removal, the residue was purified by CC (neutral Al_2O_3). White solid, 356 mg, yield 58%. Mp: 110−112 °C. ^{1}H NMR ($CDCl_3$): δ 9.66 (br s, 1H), 7.29 (t, *J* = 7.8 Hz, 1H), 7.14 (d, *J* = 7.8 Hz, 2H), 3.38 (br m, 5H), 3.14 (m, 2H), 2.38 (br m, 2H), 2.14 (s, 6H), 1.78 (br s, 2H), 1.18 (d, *J* = 6.9 Hz). ^{13}C NMR ($CDCl_3$, 50 °C): δ 185.1, 182.8, 169.2, 168.3, 146.7, 133.6, 129.1, 124.1, 55.7, 50.2, 45.5, 37.3, 25.7, 23.9, 23.7. ESI(+)-HRMS: *m*/*z* (%) calcd for $C_{22}H_{34}N_3O_2$ $[M + H]^+$ 372.2651; found 372.2660. Anal. Calcd for $C_{22}H_{33}N_3O_2$: C, 71.12; H, 8.95; N, 11.31. Found C, 71.06; H, 8.59; N, 11.23.

*3-(Diisopropylamino)-4-((3-(dimethylamino)propyl)(methyl)-amino)cyclobut-3-ene-1,2-dione (**14**).* To a solution of the squaramic acid ethyl ester **6a** (500 mg, 2.22 mmol) in EtOH (15 mL) was added *N*,*N*,*N*′-trimethyl-1,3-propanediamine (490 μL, 2.89 mmol). The mixture was stirred at 80 °C for 48 h. After solvent removal in vacuo, the residue was purified partially by CC (SiO_2; CH_2Cl_2/MeOH, 90/10 v/v) to afford an oily product. The mixture was digested four times at room temperature in a mixture of CH_2Cl_2 (1 mL) and *n*-pentane (20 mL). After decantation, to discard the insoluble material, the organic extracts were pooled and concentrated in vacuo to afford **14** as a thick oil, 350 mg, yield 53%. ^{1}H NMR ($CDCl_3$): δ 3.81 (m, 2H), 3.57 (t, *J* = 7.2 Hz, 2H), 3.11 (s, 3H), 2.27 (t, *J* = 7.2 Hz, 2H), 2.19 (s, 6H), 1.79 (m, 2H), 1.38 (d, *J* = 6.9 Hz, 12H). ^{13}C NMR ($CDCl_3$): δ 184.7, 183.6, 170.6, 170.2, 56.6, 51.2, 50.3, 45.6, 38.9, 26.1, 22.6. ESI(+)-HRMS: *m*/*z* (%) calcd for $C_{16}H_{30}N_3O_2$ $[M + H]^+$ 296.2333; found 296.2332.

NMR Experiments. A 5 mm NMR tube was loaded with ca. 3 mg of compound **10** that was then dissolved in 0.70 mL of D_2O. Then, 50 μL of a solution of NaOD (40 wt % in D_2O) was added to give a ca. 0.9 M solution of NaOD. NMR spectra were measured at room temperature immediately before and after the addition of base. The effect of base addition was as follows: ^{1}H NMR (400 MHz, 298 K, D_2O, ppm): δ 1.05 → 0.87 (t, 3H), 1.50 → 1.30 (m, 2H), 1.74 → 1.49 (m, 2H), 2.23 → 1.79 (m, 2H), 3.00 → 2.16 (s, 6H), 3.28 → 2.32 (t, 2H), 3.39 → 3.25 (s, 3H), 3.78 → 3.59 (t, 2H), 3.87 → 3.65 (br s → t).

The sample with compound **10** was kept at 37 °C for 300 min (to obtain the maximum amount of partial hydrolysis intermediate according to kinetic data) and 7 days (to achieve complete hydrolysis). The NMR spectra were compared with those of squaramides **1** and **4** and the complete hydrolysis products A + B (free amines).

^{1}H NMR (400 MHz, 298 K, D_2O, ppm): δ 0.80 (t, **1** + A), 1.26 (m, **1** + A), 1.51 (m, **1** + A), 1.73 (m, **4**), 2.07 (s, B), 2.09 (s, **4**), 2.18 (s, B), 2.23 (m, **4**+B), 2.40 (t, B), 2.49 (t, **1** + A), 3.16 (s, **4**), 3.45 (t, **1**), 3.54 (t, **4**).

Preliminary Kinetic Studies. Samples of **1**, **4** and **10** were kept at 37 °C in 10 mL vials sealed with screw caps with silicone/PTFE septa. After 0, 40, 105, and 189 days, 2 mL aliquots were taken out and measured in a Cary 50 UV−vis spectrophotometer.

Kinetic Experiments. The experiments were carried out on a Cary 50 Bio UV−vis spectrophotometer at 37.0 ± 0.1 °C (and 45, 50, 55, and 60 °C for Eyring plots) in water. Solutions of the squaramic acid

DOI: 10.1021/acs.joc.6b02963
J. Org. Chem. 2017, 82, 2160−2170

or squaramide (10^{-5} M; $\varepsilon_{max} \approx (20-30) \times 10^3$ M^{-1} cm^{-1}) were mixed with a solution of the hydroxide in a range of concentration sufficient (0.01−1.00 M) to ensure pseudo-first-order conditions. The ionic strength was kept constant through the experiments using the required amounts of the corresponding chloride salts (0.15 and 1 M). The spectral changes in the 200−900 nm range were analyzed with the program SPECFIT-32.[19]

Computational Details. DFT calculations were performed using Gaussian 09 (Revision D.01).[33] The M06-2X functional,[34] in combination with the cc-pVTZ basis set,[35] was used throughout. The effects of the solvent (H_2O, ε = 78.3553) were taken into account self-consistently through the polarizable continuum model (PCM) method.[36] All stationary points were fully characterized via analytical frequency calculations at the same level of theory as either minima (all positive eigenvalues) or transition states (one negative eigenvalue). This method also provided the corrections required to obtain the solution free energies reported in the text (298.15 K, 1 atm). IRC calculations and subsequent geometry optimizations were used to confirm the minima linked by each transition state. Regarding the calculations in the presence of an explicit H_2O molecule, in some cases the rearrangement of the tetrahedral intermediates resulting from the hydroxide attack was required before the C−N bond cleavage could take place. Nevertheless, these were found to have a small impact on their stabilities, as they mainly involved changes in the relative position of the solvent molecule. Structures were illustrated using CYLview.[37]

■ ASSOCIATED CONTENT

Supporting Information

The Supporting Information is available free of charge on the ACS Publications website at DOI: 10.1021/acs.joc.6b02963.

^1H and ^{13}C NMR spectra of new compounds, UV and ^1H NMR spectra of hydrolyzed mixtures, calculated thermodynamic data, DFT calculated structures, and Cartesian coordinates for all DFT-optimized species (PDF)

■ AUTHOR INFORMATION

Corresponding Authors

*M.G.B.: E-mail, manuel.basallote@uca.es.

*A.C.: Tel, +34 971 173266; Fax, +34 971 173426; E-mail, antoni.costa@uib.es.

ORCID

Andrés G. Algarra: 0000-0002-5062-2858

Manuel G. Basallote: 0000-0002-1802-8699

Antonio Costa: 0000-0002-9418-7798

Notes

The authors declare no competing financial interest.

■ ACKNOWLEDGMENTS

Financial support from the Spanish Ministry of Economy and Competitiveness (MINECO) (CTQ2011-27512/BQU and CONSOLIDER-INGENIO 2010 CSD2010-00065, FEDER funds) are gratefully acknowledged. M.X. thanks Govern de les Illes Balears for a predoctoral fellowship (FSE funds).

■ REFERENCES

(1) (a) Alemán, J.; Parra, A.; Jiang, H.; Jørgensen, K. A. *Chem. - Eur. J.* **2011**, *17*, 6890−6899. (b) Ian Storer, R.; Aciro, C.; Jones, L. H. *Chem. Soc. Rev.* **2011**, *40*, 2330−2346. (c) Wurm, F. R.; Klok, H.-A. *Chem. Soc. Rev.* **2013**, *42*, 8220−8236. (d) Chauhan, P.; Mahajan, S.; Kaya, U.; Hack, D.; Enders, D. *Adv. Synth. Catal.* **2015**, *357*, 253−281.

(2) (a) Ambrosi, G.; Formica, M.; Fusi, V.; Giorgi, L.; Guerri, A.; Micheloni, M.; Paoli, P.; Pontellini, R.; Rossi, P. *Chem. - Eur. J.* **2007**, *13*, 702−712. (b) Soberats, B.; Martínez, L.; Sanna, E.; Sampedro, A.; Rotger, C.; Costa, A. *Chem. - Eur. J.* **2012**, *18*, 7533−7542. (d) Qin, L.; Hartley, L. A.; Turner, P.; Elmes, R. B. P.; Jolliffe, K. A. *Chem. Sci.* **2016**, *7*, 4563−4572.

(3) (a) Yang, W.; Yang, Y.; Du, D.-M. *Org. Lett.* **2013**, *15*, 1190−1193. (b) Nair, D. K.; Menna-Barreto, R. F. S.; da Silva, E. N., Jr; Mobin, S. M.; Namboothiri, I. N. N. *Chem. Commun.* **2014**, *50*, 6973−6976. (c) Zhou, E.; Liu, B.; Dong, C. *Tetrahedron: Asymmetry* **2014**, *25*, 181−186. (d) Bera, K.; Namboothiri, I. N. N. *J. Org. Chem.* **2015**, *80*, 1402−1413. (e) Sun, Q.-S.; Zhu, H.; Chen, Y.-J.; Yang, X.-D.; Sun, X.-W.; Lin, G.-Q. *Angew. Chem., Int. Ed.* **2015**, *54*, 13253−13257.

(4) (a) Han, X.; Zhou, H.-B.; Dong, C. *Chem. Rec.* **2016**, *16*, 897−906. (b) Held, F. E.; Tsogoeva, S. B. *Catal. Sci. Technol.* **2016**, *6*, 645−667.

(5) (a) Hutchings, M. G.; Ferguson, I.; Allen, S.; Zyss, J.; Ledoux, I. *J. Chem. Res., Synop.* **1998**, 244−245. (b) Ohsedo, Y.; Miyamoto, M.; Tanaka, A.; Watanabe, H. *New J. Chem.* **2013**, *37*, 2874−2880. (c) Saez Talens, V.; Englebienne, P.; Trinh, T. T.; Noteborn, W. E. M.; Voets, I. K.; Kieltyka, R. E. *Angew. Chem., Int. Ed.* **2015**, *54*, 10502−10506.

(6) (a) Busschaert, N.; Kirby, I. L.; Young, S.; Coles, S. J.; Horton, P. N.; Light, M. E.; Gale, P. A. *Angew. Chem., Int. Ed.* **2012**, *51*, 4426−4430. (b) Busschaert, N.; Elmes, R. B. P.; Czech, D. D.; Wu, X.; Kirby, I. L.; Peck, E. M.; Hendzel, K. D.; Shaw, S. K.; Chan, B.; Smith, B. D.; Jolliffe, K. A.; Gale, P. A. *Chem. Sci.* **2014**, *5*, 3617−3626. (c) Deng, L.-Q.; Lu, Y.-M.; Zhou, C.-Q.; Chen, J.-X.; Wang, B.; Chen, W.-H. *Bioorg. Med. Chem. Lett.* **2014**, *24*, 2859−2862. (d) Wu, X.; Busschaert, N.; Wells, N. J.; Jiang, Y.-B.; Gale, P. A. *J. Am. Chem. Soc.* **2015**, *137*, 1476−1484.

(7) (a) Tomàs, S.; Prohens, R.; Deslongchamps, G.; Ballester, P.; Costa, A. *Angew. Chem., Int. Ed.* **1999**, *38*, 2208−2211. (b) Rostami, A.; Wei, C. J.; Guérin, G.; Taylor, M. S. *Angew. Chem., Int. Ed.* **2011**, *50*, 2059−2062. (c) Elmes, R. B. P.; Turner, P.; Jolliffe, K. A. *Org. Lett.* **2013**, *15*, 5638−5641. (d) Manesiotis, P.; Riley, A.; Bollen, B. *J. Mater. Chem. C* **2014**, *2*, 8990−8995.

(8) (a) Rudd, S. E.; Roselt, P.; Cullinane, C.; Hicks, R. J.; Donnelly, P. S. *Chem. Commun.* **2016**, *52*, 11889−11892. (b) Sampedro, A.; Villalonga-Planells, R.; Vega, M.; Ramis, G.; Fernández de Mattos, S.; Villalonga, P.; Costa, A.; Rotger, C. *Bioconjugate Chem.* **2014**, *25*, 1537−1546.

(9) (a) Grabosch, C.; Hartmann, M.; Schmidt-Lassen, J.; Lindhorst, T. K. *ChemBioChem* **2011**, *12*, 1066−1074. (b) Schieber, C.; Bestetti, A.; Lim, J. P.; Ryan, A. D.; Nguyen, T.-L.; Eldridge, R.; White, A. R.; Gleeson, P. A.; Donnelly, P. S.; Williams, S. J.; Mulvaney, P. *Angew. Chem., Int. Ed.* **2012**, *51*, 10523−10527. (c) Vaillant, O.; Cheikh, K. E.; Warther, D.; Brevet, D.; Maynadier, M.; Bouffard, E.; Salgues, F.; Jeanjean, A.; Puche, P.; Mazerolles, C.; Maillard, P.; Mongin, O.; Blanchard-Desce, M.; Raehm, L.; Rébillard, X.; Durand, J.-O.; Gary-Bobo, M.; Morère, A.; Garcia, M. *Angew. Chem., Int. Ed.* **2015**, *54*, 5952−5956. (d) Palitzsch, B.; Gaidzik, N.; Stergiou, N.; Stahn, S.; Hartmann, S.; Gerlitzki, B.; Teusch, N.; Flemming, P.; Schmitt, E.; Kunz, H. *Angew. Chem., Int. Ed.* **2016**, *55*, 2894−2898.

(10) (a) Kinney, W. A.; Abou-Gharbia, M.; Garrison, D. T.; Schmid, J.; Kowal, D. M.; Bramlett, D. R.; Miller, T. L.; Tasse, R. P.; Zaleska, M. M.; Moyer, J. A. *J. Med. Chem.* **1998**, *41*, 236−246. (b) Sato, K.; Seio, K.; Sekine, M. *J. Am. Chem. Soc.* **2002**, *124*, 12715−12724. (c) Lee, C.-W.; Cao, H.; Ichiyama, K.; Rana, T. M. *Bioorg. Med. Chem. Lett.* **2005**, *15*, 4243−4246. (d) Seio, K.; Miyashita, T.; Sato, K.; Sekine, M. *Eur. J. Org. Chem.* **2005**, *2005*, 5163−5170.

(11) (a) Villalonga, P.; Fernández de Mattos, S.; Ramis, G.; Obrador-Hevia, A.; Sampedro, Á.; Rotger, C.; Costa, A. *ChemMedChem* **2012**, *7*, 1472−1480. (b) Fernandez-Moreira, V.; Alegre-Requena, J. V.; Herrera, R. P.; Marzo, I.; Gimeno, M. C. *RSC Adv.* **2016**, *6*, 14171−14177. (c) Quintana, M.; Alegre-Requena, J. V.; Marques-Lopez, E.; Herrera, R. P.; Triola, G. *MedChemComm* **2016**, *7*, 550−561.

(12) (a) Kumar, S. P.; Gloria, P. M. C.; Goncalves, L. M.; Gut, J.; Rosenthal, P. J.; Moreira, R.; Santos, M. M. M. *MedChemComm* **2012**, *3*, 489−493. (b) Olmo, F.; Rotger, C.; Ramírez-Macías, I.; Martínez, L.; Marín, C.; Carreras, L.; Urbanová, K.; Vega, M.; Chaves-Lemaur, G.; Sampedro, Á.; Rosales, M. J.; Sánchez-Moreno, M.; Costa, A. *J.*

Med. Chem. **2014**, *57*, 987−999. (c) Ribeiro, C. J. A.; Espadinha, M.; Machado, M.; Gut, J.; Gonçalves, L. M.; Rosenthal, P. J.; Prudêncio, M.; Moreira, R.; Santos, M. M. M. *Bioorg. Med. Chem.* **2016**, *24*, 1786−1792.
(13) Rotger, C.; Soberats, B.; Quiñonero, D.; Frontera, A.; Ballester, P.; Benet-Buchholz, J.; Deyà, P. M.; Costa, A. *Eur. J. Org. Chem.* **2008**, *2008*, 1864−1868.
(14) Rotger, C.; Piña, M. N.; Frontera, A.; Martorell, G.; Ballester, P.; Deyà, P. M.; Costa, A. *J. Org. Chem.* **2004**, *69*, 2302−2308.
(15) Quiñonero, D.; Garau, C.; Frontera, A.; Ballester, P.; Costa, A.; Deyà, P. M. *Chem. - Eur. J.* **2002**, *8*, 433−438.
(16) Prohens, R.; Tomàs, S.; Morey, J.; Deyà, P. M.; Ballester, P.; Costa, A. *Tetrahedron Lett.* **1998**, *39*, 1063−1066.
(17) Tomàs, S.; Prohens, P.; Vega, M.; Rotger, M. C.; Deyà, P. M.; Ballester, P.; Costa, A. *J. Org. Chem.* **1996**, *61*, 9394−9401.
(18) (a) Cohen, S.; Cohen, S. G. *J. Am. Chem. Soc.* **1966**, *88*, 1533−1536. (b) Wurm, F.; Steinbach, T.; Klok, H.-A. *Chem. Commun.* **2013**, *49*, 7815−7817. (c) Tietze, L. F.; Schröder, C.; Gabius, S.; Brinck, U.; Goerlach-Graw, A.; Gabius, H.-J. J. *Bioconjugate Chem.* **1991**, *2*, 148−153.
(19) Binstead, R. A.; Jung, B.; Zuberbühler, A. D. *SPECFIT-32*; Spectrum Software Associates, Chapel Hill, NC, USA, 2000.
(20) Laudien, R.; Mitzner, R. J. *Chem. Soc., Perkin Trans. 2* **2001**, 2226−2229.
(21) (a) Bruylants, A.; Kezdy, F. *Record Chem. Progr.* **1960**, *21*, 213. (b) Kezdy, F.; Bruylants, A. *Bull. Soc. Chim. Belg.* **1960**, *69*, 602−615.
(22) Biechler, S. S.; Taft, R. W. *J. Am. Chem. Soc.* **1957**, *79*, 4927−4935.
(23) Mabey, W.; Mill, T. *J. Phys. Chem. Ref. Data* **1978**, *7*, 383−415.
(24) (a) Cox, J. R.; Ramsay, O. B. *Chem. Rev.* **1964**, *64*, 317−352. (b) Williams, N. H.; Wyman, P. *Chem. Commun.* **2001**, 1268−1269.
(25) Talbot, R. J. E. The Hydrolysis of Carboxylic Acid Derivatives. In *Ester Formation and Hydrolysis and Related Reactions*; Bamford, C. H., Tipper, C. F. H., Eds.; Elsevier: Amsterdam, 1972; Comprehensive Chemical Kinetics *10*, pp 209−287.
(26) O'Connor, C. Q. *Q. Rev., Chem. Soc.* **1970**, *24*, 553−564.
(27) See, for instance: (a) Mujika, J. I.; Mercero, J. M.; Lopez, X. *J. Am. Chem. Soc.* **2005**, *127*, 4445−4453. (b) Xiong, Y.; Zhan, C.-G. *J. Phys. Chem. A* **2006**, *110*, 12644−12652. (c) Cheshmedzhieva, D.; Ilieva, S.; Hadjieva, B.; Galabov, B. *J. Phys. Org. Chem.* **2009**, *22*, 619−631 and references therein.
(28) (a) Lu, T.; Wheeler, S. E. *Chem. - Eur. J.* **2013**, *19*, 15141−15147. (b) Kótai, B.; Kardos, G.; Hamza, A.; Farkas, V.; Pápai, I.; Soós, T. *Chem. - Eur. J.* **2014**, *20*, 5631−5639.
(29) Note that once the tetrahedral intermediate is generated, it can undergo conformational isomerizations before evolving into products. See ref 27f.
(30) It is worth noting that intrinsic reaction coordinate (IRC) calculations at $\mathbf{TS_2(5)}$ followed by structure optimization also lead to the H-bonded squarate dianion and phenylamine compounds.
(31) Phenylamine has a pK_b values that is ca. 6 units larger than that of *n*-butylamine. See: Silberberg, M. In *Principles of General Chemistry*, 3rd ed.; McGraw-Hill Higher Education: Burr Ridge, IL, USA, 2012.
(32) López, C.; Vega, M.; Sanna, E.; Rotger, C.; Costa, A. *RSC Adv.* **2013**, *3*, 7249−7253.
(33) Frisch, J.; Trucks, G. W.; Schlegel, H. B.; Scuseria, G. E.; Robb, M. A.; Cheeseman, J. R.; Scalmani, G.; Barone, V.; Mennucci, B.; Petersson, G. A.; Nakatsuji, H.; Caricato, M.; Li, X.; Hratchian, H. P.; Izmaylov, A. F.; Bloino, J.; Zheng, G.; Sonnenberg, J. L.; Hada, M.; Ehara, M.; Toyota, K.; Fukuda, R.; Hasegawa, J.; Ishida, M.; Nakajima, T.; Honda, Y.; Kitao, O.; Nakai, H.; Vreven, T.; Montgomery, J. A., Jr.; Peralta, J. E.; Ogliaro, F.; Bearpark, M.; Heyd, J. J.; Brothers, E.; Kudin, K. N.; Staroverov, V. N.; Kobayashi, R.; Normand, J.; Raghavachari, K.; Rendell, A.; Burant, J. C.; Iyengar, S. S.; Tomasi, J.; Cossi, M.; Rega, N.; Millam, J. M.; Klene, M.; Knox, J. E.; Cross, J. B.; Bakken, V.; Adamo, C.; Jaramillo, J.; Gomperts, R.; Stratmann, R. E.; Yazyev, O.; Austin, A. J.; Cammi, R.; Pomelli, C.; Ochterski, J. W.; Martin, R. L.; Morokuma, K.; Zakrzewski, V. G.; Voth, G. A.; Salvador, P.; Dannenberg, J. J.; Dapprich, S.; Daniels, A. D.; Farkas, Ö.; Foresman, J. B.; Ortiz, J. V.; Cioslowski, J.; Fox, D. J. *Gaussian 09 (Revision D.01)*; Gaussian, Inc., Wallingford, CT, 2009.
(34) Zhao, Y.; Truhlar, D. G. *Theor. Chem. Acc.* **2008**, *120*, 215−241.
(35) Woon, D. E.; Dunning, T. H. *J. Chem. Phys.* **1995**, *103*, 4572−4585.
(36) (a) Cossi, M.; Scalmani, G.; Rega, N.; Barone, V. *J. Chem. Phys.* **2002**, *117*, 43−54. (b) Tomasi, J.; Mennucci, B.; Cammi, R. *Chem. Rev.* **2005**, *105*, 2999−3093.
(37) Legault, C. *CYLview v1.0b*; Université de Sherbrooke, Sherbrooke, Canada, 2009.
(38) Niewiadomski, S.; Beebeejaun, Z.; Denton, H.; Smith, T. K.; Morris, R. J.; Wagner, G. K. *Org. Biomol. Chem.* **2010**, *8*, 3488−99.
(39) Jin, C.; Zhang, M.; Deng, C.; Guan, Y.; Gong, J.; Zhu, D.; Pan, Y.; Jiang, J.; Wang, L. *Tetrahedron Lett.* **2013**, *54*, 796−801.
(40) Ehrhardt, H.; Hünig, S.; Pütter, H. *Chem. Ber.* **1977**, *110*, 2506−2523.

DOI: 10.1021/acs.joc.6b02963
J. Org. Chem. 2017, 82, 2160−2170